# 3,4′-Dihydroxybenzophenone Terephthalate: An All-Aromatic Thermotropic Polyester with a Helical Chain Conformation

**R. S. Irwin and W. Sweeny**

*Textile Fibers Department, E. I. du Pont de Nemours & Co., Experimental Station, Wilmington, Delaware 19898*

**K. H. Gardner, C. R. Gochanour,* and M. Weinberg**

*Central Research and Development Department, E. I. du Pont de Nemours & Co., Experimental Station, Wilmington, Delaware 19898.* *Received January 13, 1988*

ABSTRACT: Polymers which form nematic melts are usually prepared from 1,4-substituted aromatic intermediates, e.g., *p*-hydroxybenzoic acid or *p*-aminobenzoic acid, to obtain a rod- or ribbonlike conformation. This paper describes the preparation, structure, and properties of a liquid crystalline aromatic polyester that exists in a helical conformation in the solid state and an extended conformation in the nematic phase. Surprisingly, fiber tensile properties are in the same range as those for many rigid-rod polymers. The polymer is prepared from 3,4′-dihydroxybenzophenone and terephthalic acid. The polymer can be highly crystalline and has a crystal to nematic transition at 285 °C and a sharp nematic to isotropic transition at 360 °C. The phase behavior has been characterized by DSC and rheological techniques. The unique properties of 3,4′-dihydroxybenzohenone terephthalate (3,4′PCOPG-T) are a result of the conformational degrees of freedom of the chain. The 3,4′-dihydroxybenzophenone unit can have either an extended or bent conformation. In the solid state, an extended conformation is adopted, resulting in a 4-fold helical conformation with a fiber repeat of 6.76 nm. The results of a detailed X-ray study of this structure and of the structure of amorphous fibers are discussed. Although the structure of this polyester is considerably different than that normally found in liquid crystal polyesters, fibers of 3,4′PCOPG-T show good tensile properties. The dependence of tensile properties on thermal history has been determined and the relative contributions of crystallinity and molecular weight growth to the tensile properties are discussed.

## Introduction

Liquid crystalline phases are found in a wide variety of polymer systems including both solution and melt. Although phases with higher order, e.g., smectic, have been reported, the most common liquid crystalline phase observed in polymers is nematic. The general requirement for the existence of a nematic phase is that the polymer must be rodlike over a sufficiently long distance.[1] Then, above a critical volume fraction, steric constraints favor the formation of the ordered state.

A number of strategies have been employed to obtain rodlike structures, including rigid units incorporated either as side chains or as components in the main chain with or without a flexible spacer.[2] One class that has been studied in great detail is that based on 1,4-substituted aromatic intermediates, such as *p*-aminobenzoic acid, terephthalic acid, *p*-phenylenediamine, and *p*-hydroxybenzoic acid.[2b,3] The chain conformation in these polymers is essentially rodlike due to planar trans conformation of the amide or ester linkage.[4] This type of structure has lead to polymers with superior mechanical properties.

In this paper we describe the preparation and properties of a unique thermotropic polyester derived from 3,4′-dihydroxybenzophenone (3,4′PCOPG) and terephthalic acid (T). The structures of the monomers are shown in Figure 1. This polyester is different from other all-aromatic polyesters in two ways. First, the substituted benzophenone is not symmetric and can be incorporated in two manners, T-34′-T or T-4′3-T. As a result the chain will be composed of segments which are incorporated randomly or in a regular fashion. The two simplest regular configurations, shown in Figure 2, are head-to-tail (T-34′-T-34′-T-34′-T) and head-to-head (T-34′-T-4′3-T-34′-T). Second, two equal energy conformations exist for the 3,4′PCOPG monomer. As shown in Figure 3, either an extended trans conformation or a bent cis conformation can be adopted. The crucial difference between the two conformations is the effect on chain trajectory; the other details of the conformation are not important. The cis and trans nomenclature was chosen to emplasize this difference. There is no reason for either conformation to be preferred in isotropic phases. In the absence of order, the chain conformation found in the melt will be essentially identical with that found in dilute solution under Θ conditions. However, recent theoretical models predict that this will not be the case in a nematic phase.[5] Excluded-volume interactions in the ordered phase result in a strong preference for linear or rodlike conformations. The 3,4′PCOPG-T chain appears to be a good system in which to test these predictions because the chain can adopt either the extended trans or bent cis conformation.

X-ray studies of this polymer indicate that the chain conformation in the most stable crystalline state is helical and extended. To our knowledge this is the first helical fully aromatic thermotropic polyester. Because of disorder due to the nonsymmetric 3,4′PCOPG moiety, the helical structure does not encompass the entire chain. Initially, crystallites are formed from existing runs with the proper configuration; solid-phase polymerization results in an increase in run length and crystallite size. Diffraction studies of noncrystalline fibers demonstrate that the chain is predominately made up of extended trans conformations. Thus although this chain is quite flexible in isotropic phases, a rodlike conformation is found in the nematic phase.

Finally, this polymer is of interest because of the existence of a sharp nematic to isotropic transition which occurs at approximately 360 °C. Although a number of nematic melts exhibit nematic to isotropic transitions, the transition generally occurs over a wide temperature range. For 3,4′PCOPG-T, the transition occurs over a narrow range and can be characterized experimentally.

In this paper we report on the preparation, crystal structure, thermal properties, fiber spinning, and fiber mechanical properties for 3,4′PCOPG-T and the rela-

* Author to whom correspondence should be addressed.

0024-9297/89/2222-1065$01.50/0 

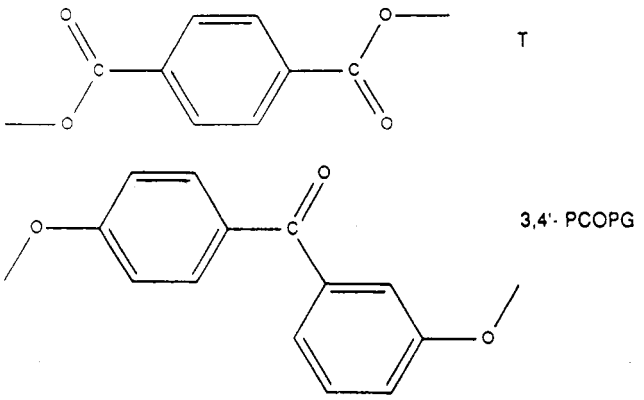


**Figure 1.** Structure of the monomers used, terephthalic acid (T) and 3,4′-dihydroxybenzophenone (3,4′PCOPG).

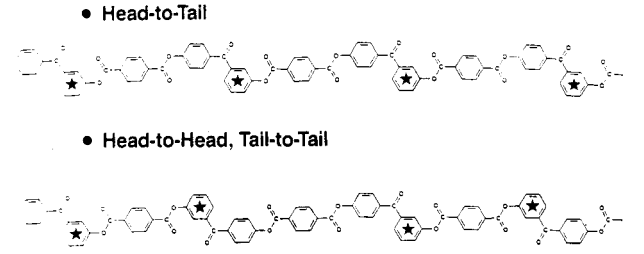


**Figure 2.** Two possible regular modes of incorporation of the nonsymmetric 3,4′PCOPG segment within the polymer chain. The 4′-end of each 3,4′PCOPG unit is indicated with a star. Although the extension of the chain is the same for both modes, the chains are not identical.

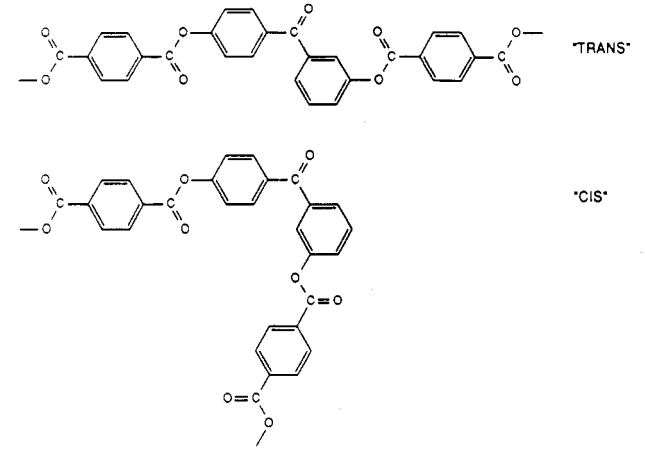


**Figure 3.** Two possible conformations of the 3,4′PCOPG segment. The trans conformer is extended while the cis conformer results in a kink in the chain imparting substantial flexibility.

tionship of these properties to the chain structure.

## Experimental Section

The aromatic diol (3,4′PCOPG) was prepared by reacting *m*-hydroxybenzoic acid (110 g) with phenol (80 g) in HF (500 g) at 30 °C under a pressure of 30 psi $BF_3$ in a Hastelloy autoclave for 4 h. The $BF_3$ and HF were then vented and the mixture was poured over ice (2 kg). The product was washed with water, 5% aqueous $NaHCO_3$, and water again before drying under vacuum at 80 °C (yield 163 g). The diacetate was prepared from the diol by refluxing for 4 h with acetic anhydride (3× weight) and concentrated $H_2SO_4$ (6 drops). The reaction mixture was poured into ice water (2 kg) and the solid precipitate filtered and dried under vacuum at 60 °C. Recrystallization from methanol yielded the diacetate (187 g) as colorless crystals, mp 84.5 °C.

The diol was obtained from the purified diacetate (149 g) by refluxing overnight in ethanol (500 mL) and trifluoromethanesulfonic acid (0.8 mL). Ethyl acetate was slowly removed by distillation through a 12-in. Vigreaux column. Ethanol was then removed by distillation to yield a final volume of 250 mL. The product was precipitated by the addition of water (250 mL). After filtration, the off-white solid was recrystallized from boiling ethanol and dried under vacuum to yield white needles with mp 203 °C.

Three methods of polymerization were used to prepare 3,4′PCOPG-T and copolymers with small amounts of resorcinol.[6] The procedures described are for the preparation of the homopolymer; similar procedures were used to prepare the copolymers.[7] The standard method of polymerization used was acidolysis. The polymerization was carried out by heating 3,4′PCOPG diacetate (29.8 g), terephthalic acid (16.6 g), and (dimethylamino)pyridine (0.005 g) in a flask equipped with a distillation head, column, and inert gas sweep. The flask was heated in a 340 °C Woods metal bath and stirred rapidly during the reaction. Acetic acid was removed through the distillation column; approximately 10 mL (80%) was collected in the first 15 min of the polymerization. The mixture was heated for a total of 20 min at atmospheric pressure followed by 25 min under 0.5-mm vacuum and then allowed to cool. A similar procedure was used to prepare the polymer by phenyl ester exchange. In this method 3,4′PCOPG (42.8 g) was reacted with diphenyl terephthalate (63.6 g) and (dimethylamino)pyridine (0.02 g). The mixture was stirred at 250 °C for 30 min, 275 °C for 15 min, 300 °C for 30 min, and 340 °C for 30 min. During these heating periods phenol was removed as the distillate. Finally, the mixture was heated under 2-mm vacuum at 340 °C for 3 h. The final polymerization technique used was a low-temperature solution process. In the procedure the 3,4′PCOPG (30.45 g) was dissolved in dry *N*-methylpyrrolidone (400 mL). The solution was cooled to ~10 °C and then dry distilled triethylamine (40 g) added. Terephthaloyl chloride (30.45 g) in methylene chloride was then added with rapid stirring. The temperature of the mixture rapidly reached about 50 °C and a solid yellow mush was formed. After standing overnight at room temperature, the polymer was dispersed in water, washed extensively with hot water, and dried under vacuum at 100 °C. The polymer prepared by each of these three methods was characterized by its inherent viscosity, measured at 0.5% concentration in pentafluorophenol. Inherent viscosities within a range 0.4 to 2 dL/g were obtained.

Hydroxyl end groups were determined by reaction of the polymer in hot nitrobenzene with dinitrobenzoyl chloride followed by back-titration with ethanolic KOH. Carboxyl end groups were measured in hot *o*-cresol by titration with *tert*-butylammonium hydroxide in isopropyl alcohol.

Fibers were spun by using a pressure spinner or screw melter with a cell temperature of about 315 °C and a spinneret temperature of about 330 °C. Fibers were typically spun at 900 m/min with a 15 × 30 mil single-hole spinneret or at 350 m/min with a 34-hole 9 × 12 mil spinneret.

DSC data were obtained by using a Mettler DSC 30 with a heating rate of 20 °C/min. A constant flow of dry nitrogen was maintained during all runs.

X-ray fiber diffraction patterns were obtained from single filaments and small bundles of fibers by using Ni-filtered Cu K$\alpha$ radiation and a 57.3-mm radius vacuum cyclindrical camera. Diffraction patterns were digitized with a Photomation P1700 rotating drum film scanner (Optronics) and processed on a AED767 raster graphics terminal using the Fiber Diffraction Processing Program (FDPP).[8]

Meridional and equatorial wide-angle X-ray diffraction scans were obtained by using a Philips X-ray diffractometer (symmetrical transmission mode, curved crystal monochrometer, pulse height analyzer, divergence and receiving slits, 1°) and Cu K$\alpha$ radiation. For these experiments the fiber was wrapped around a frame to produce a flat, parallel array of filaments 0.35 mm thick. Typically, data were collected in a fixed time mode with a step size of 0.02° 2$\theta$ and run from 3° to 60° 2$\theta$. Background scattering was fit with a cubic spline function and removed. The remaining pattern was fit with one or more Gaussian peaks that were defined by the refinable parameters—height, position, breadth. Instrumental broadening was measured by using the strong reflection at 28.46° 2$\theta$ from an annealed silicon powder (NBS-640A) and found to be 0.19°. The crystalline persistence lengths in directions parallel and perpendicular to the fiber axis were estimated by using the breadths of the 004 and 110 reflections (after correction for instrumental broadening) in the Scherrer equation.[9]

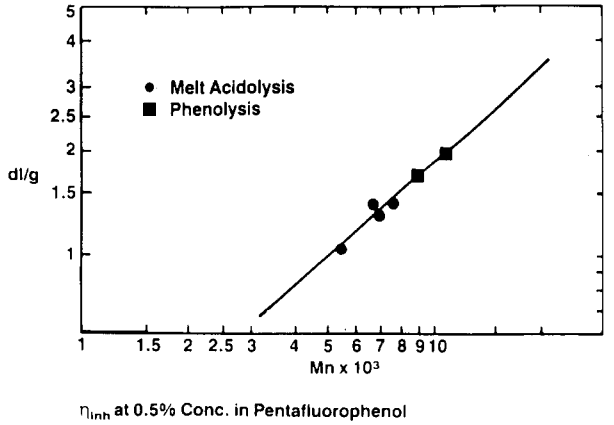


**Figure 4.** Dependence of inherent viscosity (measured at 0.5% concentration in pentafluorophenol) on $M_n$ for 3,4′PCOPG-T. The power law exponent is approximately 0.9.

The rheological properties of the polymer were measured with an Instron Model 3211 constant-velocity capillary rheometer. The capillary used in these experiments had a length of 5.1 cm and diameter 0.0744 cm($L/D$ = 68). A large $L/D$ capillary was chosen to minimize the effect of entrance and exit pressure drops. The apparent viscosity and shear rate were calculated by using standard formulas; no corrections were applied. Temperatures quoted were measured with thermocouples mounted in the rheometer barrel and are accurate to ~5 °C. To minimize polymer degradation at high temperature the rheometer barrel was flushed with nitrogen during filling. In addition, the dependence of viscosity on shear rate was determined by measuring the points in random order rather than by increasing or decreasing the shear rate throughout the range studied to avoid any systematic error due to small amounts of decomposition.

Fiber tensile properties were measured by using an Instron tensile tester. An elongation rate of 10%/min was used; the value of the initial modulus reported was determined from the stress–strain data from 1 to 10% of the breaking stress.

The compressive strength was measured by using a method in which the fiber is subjected to compressive strains on recoil from tension.[10] The energy stored in the fiber during a tensile test is converted to compressive stresses when the fiber recoils after being cut. Compressive failure is judged to occur by the appearance of kink bands.

## Results and Discussion

**Polymer Properties and Melt Structure.** The relationship between number-average molecular weight, determined by end-group analysis, and inherent viscosity is shown in Figure 4. The power law exponent obtained, 0.9, is consistent with a chain structure which is, at least on long length scales, quite flexible.[11]

A representative DSC trace for 3,4′PCOPG-T prepared by melt acidolysis is shown in Figure 5. The transitions observed are the glass transition at 100 °C, crystallization at about 180 °C, crystal to nematic at 285 °C, and nematic to isotropic at 360 °C. The identification of the crystal to nematic and nematic to isotropic transitions was confirmed by optical microscopy. The DSC results are summarized in Table I. The melting temperature and heat of fusion are dependent on the thermal history of the sample, with high crystallinity only found in samples annealed at high temperature. In contrast, the nematic to isotropic transition temperature and enthalpy are independent of the sample history. This annealing process and its affect on mechanical properties will be discussed in more detail in a later section.

A unique feature of 3,4′PCOPG-T is the presence of a sharp nematic to isotropic transition. In most all aromatic main-chain nematic polymers the decomposition temperature is reached before the nematic to isotropic transition occurs. This is in large part due to the very rigid structures

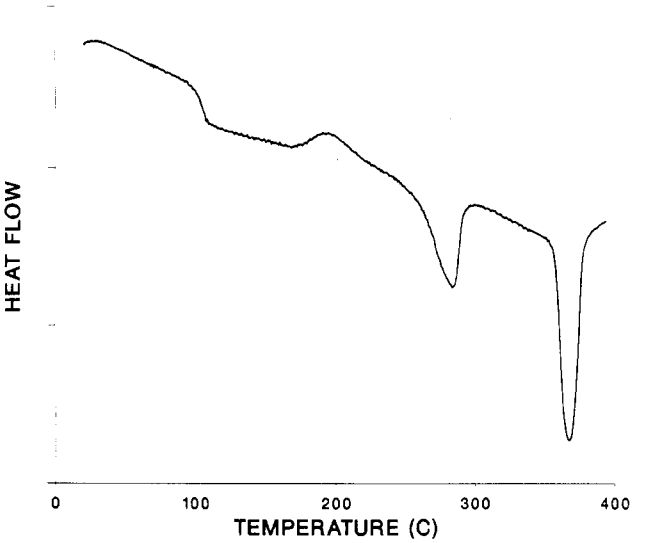


**Figure 5.** DSC scan for the as-polymerized 3,4′PCOPG-T flake. The data shown were obtained on a second heating cycle at 20 °C/min heating rate.

**Table I**
**DSC Results: 3,4′PCOPG-T**

| sample description | $T_{KN}$, °C | $\Delta H_{KN}$, cal/g | $T_{NI}$, °C | $\Delta H_{NI}$, cal/g |
|---|---|---|---|---|
| melt polymerized | 282 | 3.6 | 353 | 5.3 |
| solution polymerized | 276 | 2.6 | 360 | 5.5 |
| as-spun fiber | 282 | 2.4 | 348 | 5.0 |
| heat-treated fiber[a] | 276 | 3.1 | 368 | 4.3 |
| solid-phase polymerized[b] | 320 | 10.3 | 378 | 4.8 |

[a] Annealed at 190 °C for 60 h. Similar results were found for shorter annealing times. [b] Annealed at 190 °C for 3 h and 280 °C for 48 h.

generally studied. In systems which are modified to reduce chain stiffness by incorporation of a comonomer, e.g., *p*-hydroxybenzoic acid/poly(ethylene terephthalate) copolymers, regimes of composition exist where nematic and isotropic phases coexist over a wide temperature range. The transition behavior of 3,4′PCOPG-T is similar to that found for small molecule nematics, side-chain polymer nematics, and flexible spacer polymer nematics rather than main-chain nematics. The enthalpy change at the nematic to isotropic transition is approximately 5 cal/g; the entropy change is 2.5 cal/(K mol of chemical repeat). When compared to small molecule nematics this value for the entropy change is quite large. For small molecule nematics typical values of $\Delta S$ fall within the range 0.5–1 cal/(K mol).[12] A likely explanation for the large value of $\Delta S$ is that a conformational change accompanies the transition.[13] Recent theoretical models predict that linear or rodlike conformations are preferred in the nematic state.[5] The nematic to isotropic transition is then coupled to a conformation change in which this preference for rodlike conformations is relaxed. For 3,4′PCOPG-T this would mean that cis conformations would be largely excluded in the nematic phase but allowed in the isotropic phase.

The melt structure and phase transitions have a direct effect on the properties of the melt. In Figure 6 flow curves for 3,4′PCOPG-T are shown as a function of temperature. The temperature range covered (320–400 °C) includes regions where the melt is a single-phase nematic and the nematic to isotropic transition region.[14] The dependence of viscosity on shear rate is similar for all temperatures; there is no obvious indication of the phase transition, i.e., the flow curves all look quite similar. The magnitude of the viscosity does, however, show a dramatic dependence

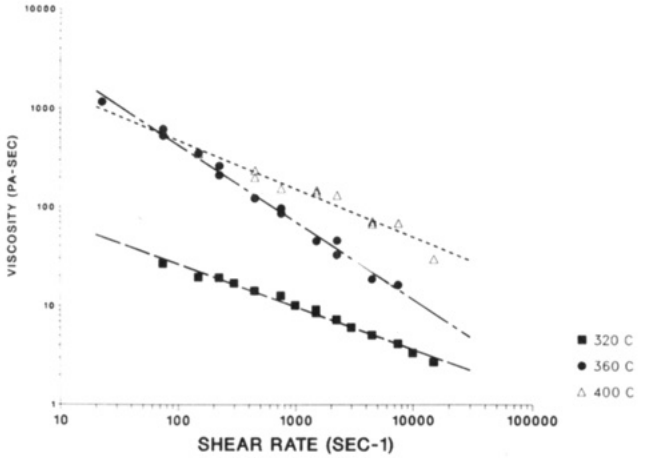


**Figure 6.** Temperature-dependent flow curves for 3,4′PCOPG-T. For all temperatures studied, the melt is a power law fluid. The temperature range extends over the range where the nematic to isotropic transition occurs.

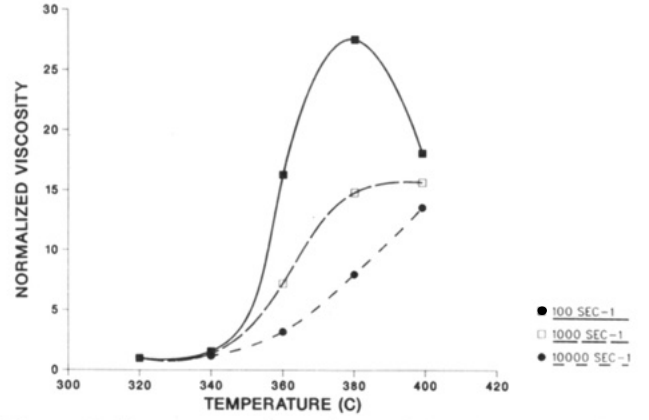


**Figure 7.** Temperature dependence of viscosity measured at constant shear rate. For the lowest shear rate studied there is a maximum in the viscosity near the nematic to isotropic transition. This maximum shifts to higher temperature with increasing shear rate.

on temperature. In Figure 7 the viscosity is shown as a function of temperature at constant shear rate. Values of $\dot{\gamma}$ of 100, 1000, and 10 000 $s^{-1}$ were arbitrarily chosen to cover the range of shear rates studied.[15] The values plotted are normalized to the viscosity for that shear rate at 320 °C. At low shear rate (100 $s^{-1}$), we find that the viscosity increases with temperature from 320 to 380 °C and then decreases at higher temperature. This temperature dependence is qualitatively what would be expected.[16] An increase in viscosity would be expected as a second phase (isotropic) is added to the nematic phase. Eventually phase inversion (continuous phase isotropic) occurs. The viscosity then begins to decrease as the amount of the second phase (now anisotropic) decreases with increasing temperature. An analogous change with concentration has been reported for lyotropic systems, such as aromatic polyamides.[17] As the shear rate is increased the temperature at which the maximum in viscosity occurs shifts to higher temperature. This shift results in a curve with a plateaulike shape at 1000 $s^{-1}$. Presumably the viscosity would decrease again at higher temperature. At 10 000 $s^{-1}$ the viscosity is a monotonically increasing function of temperature. These variations in the viscosity maximum with shear rate reflect the orientation produced with increasing shear. The clearing temperature is shifted to increasing temperature with increasing shear rate, indicating a stabilization of the nematic state by shear. A final point which should be noted is that for all shear rates

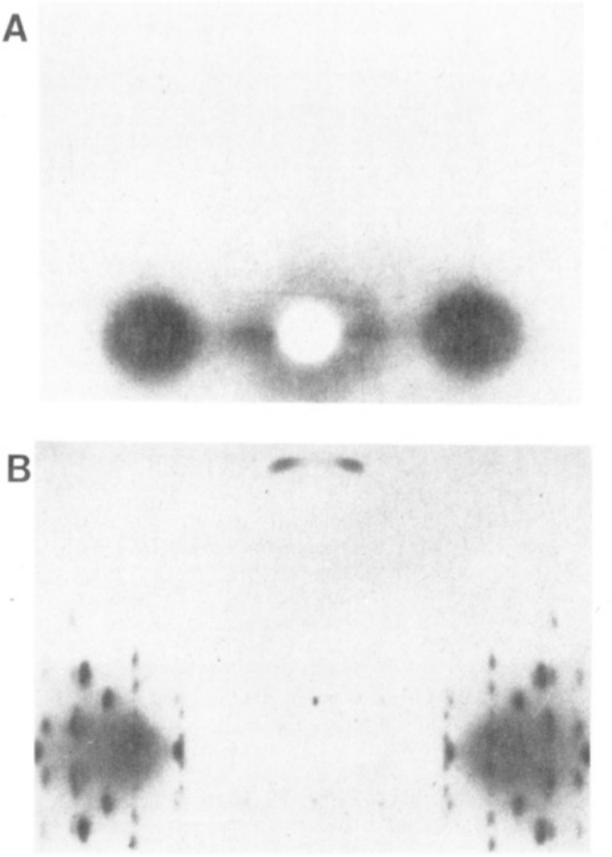


**Figure 8.** Fiber diffraction patterns for (A) as-spun and (B) heat-treated (190 °C/3 h) 3,4′PCOPG-T fiber. The fiber axis is vertical. The as-spun fiber is oriented and noncrystalline. Heat treatment results in a fiber with substantial crystallinity.

shown, there is an increase in viscosity with temperature from 320 to 340 °C. The viscosity is 1.2–1.5 times the value at 320 °C. This is somewhat surprising in view of the DSC data, where the nematic to isotropic transition begins at 340 °C. Although it is possible that the increase in viscosity is due to the presence of a second phase (isotropic or crystalline), another plausible explanation can be advanced. For small molecule nematics the order parameter drops rapidly with increasing temperature near the clearing temperature.[18] The increase in viscosity which we observe from 320 to 340 °C may reflect a decrease in the order parameter over this range.

**Fiber Properties.** The presence of nematic order in a polymer melt or solution results in the facile production of orientation which is especially useful in preparing high-performance fibers.[19] The X-ray diffraction pattern of an as-spun 3,4′PCOPG-T fiber, shown in Figure 8A, indicates that a noncrystalline and highly oriented fiber is produced. Typical tensile properties found for as-spun fibers were a tenacity of 1 to 1.5 GPa, initial modulus of about 50 GPa, and extension to break of 3.6%.

Substantial improvement in the tensile properties of 34′PCOPG-T (and other thermotropic polyester) fibers can be achieved by high temperature heat treatment.[20] Both physical and chemical changes can be expected to occur upon heat treatment, including crystallization, improvement of crystalline perfection, molecular weight growth, or changes in sequence distribution. The diffraction pattern of melt polymerized 34′PCOPG-T heat treated at 280 °C for 10 h shows high crystallinity and orientation. Table II lists representative tensile properties for heat-treated samples. The highest properties are obtained by annealing for 10 h at temperatures near the melting tem-

**Table II**
**Mechanical Properties of 3,4′PCOPG-T Fibers**

| prep conditns | $T/E/M^a$ | structure |
|---|---|---|
| as-spun | 1.5/3.7/50 | amorphous, oriented |
| 190 °C, 3 h | 1.7/3.8/48 | crystalline, oriented |
| 280 °C, 10 h | 4.3/7.0/57 | crystalline, oriented |
| 280 °C, 10 h[b] | 4.6/4.7/77 | crystalline, oriented |
| 350 °C, 10 h | 0.5/8.0/7.3 | amorphous, unoriented |

[a] Tensile strength (GPa)/elongation at break (%)/initial modulus (GPa). [b] This sample was a 10-in. yarn composed of 30 filaments. The remainder of the results are for 1 in single filaments.

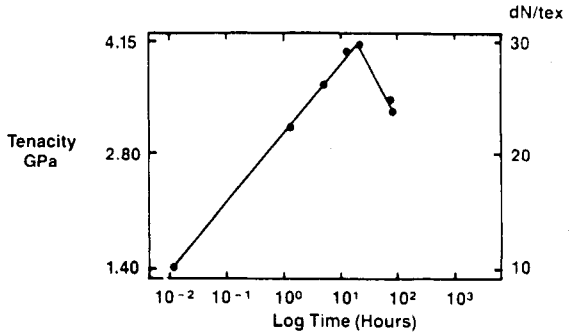


**Figure 9.** The effect of heat treatment (280 °C) on tensile strength. The tensile strength increases with time as molecular weight growth occurs. The decline in properties at very long times is probably due to degradation.

perature of the polymer. The tensile strength increases by about a factor of 3 to 4.3 GPa. The large value for the elongation to break for 1-in. single filament samples is an artifact due to Instron grip slippage. The elongation to break in 10-in. yarn samples is 4.5%, while the modulus increases by about 50% to 75 GPa. The toughness of 3,4′PCOPG-T fibers is about 2× that found for commercially available Kevlar fibers. In Figure 9, the dependence of the tenacity on heating time at 280 °C is shown; the tenacity increases rapidly at short times, reaches a peak value of about 4 GPa, and then decreases with further annealing. The diffraction pattern of 3,4′PCOPG-T heat treated for 3 h at 190 °C shows that the fibers are crystalline and demonstrates that crystallization of as-spun fibers occurs at much lower temperatures than required for heat strengthening. Measurements of the mechanical properties of these fibers (Table II) indicate only a slight change in fiber properties. This clearly shows that it is molecular weight buildup and not crystallinity that produces major enhancement in fiber properties on heat treament. It is well-known that the molecular weight of polyesters can be increased above the value obtained at melt equilibrium by solid-phase polymerization. Finally, increasing the annealing temperature to 350 °C results in a sharp decline in properties, due both to a loss of orientation and degradation. The time scale over which the tenacity change occurs on heat strengthening is similar to that found for molecular weight growth by solid-phase polymerization. Empirically it has been found for a number of polymers that a plot of the inverse of tenacity is linear when plotted versus the inverse of inherent viscosity[21] (~proportional to molecular weight for 3,4′PCOPG-T). This type of plot is shown in Figure 10. The results shown are obtained from the tenacity of as-spun fibers for different inherent polymers. It is clear that the tenacity and molecular weight are strongly correlated. The intercept, i.e., the expected strength at infinite molecular weight, is about 5.5 GPa. The mechanism of solid-state polymerization involves the concentrating chain ends in the amorphous phase followed by polymerization and removal of low molecular weight by-products.[22] The

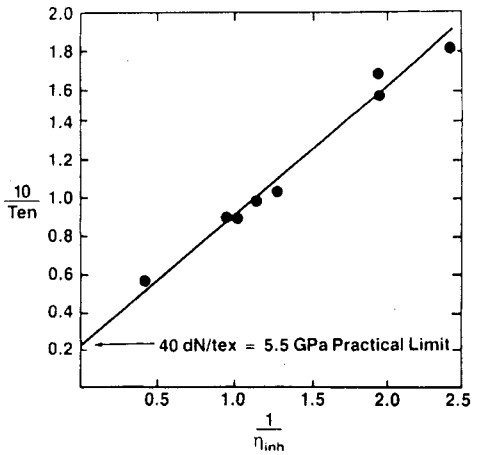


**Figure 10.** The dependence of tensile strength on molecular weight for as-spun fiber. The data are plotted as the inverse of tensile strength and the inverse of inherent viscosity. As expected, there is an improvement in properties with increasing molecular weight. The extrapolated tensile strength predicted for infinite molecular weight is 5.5 GPa.

**Table III**
**Dependence of Fiber Properties on Synthesis Method**

| | tensile strength, GPa | | |
|---|---|---|---|
| | acetates | phenyl ester | low temp |
| as spun | 1.06 | 1.13 | 0.67 |
| heat treated[a] | 1.68 | 2.07 | 1.02 |
| heat treated with KI catalyst[a] | 2.36 | 2.44 | 0.77 |

[a] 0.5 h at 280 °C.

rate of reaction can be catalyzed with KI[23] (topically applied from 0.5% ethanolic solution). The rate of chain end removal and molecular weight growth will therefore depend on the degree of crystallinity and on the chemical nature of the ends available for reaction. The results in Table III demonstrate the importance of these factors in the heat strengthening process. Both acidolysis and phenyl ester exchange (melt polymerizations) show about a 2× increase in tenacity within 1 h at 280 °C, while the low-temperature polymer approaches high strength much more slowly. Several differences between melt polymer and low-temperature solution polymer could account for this difference in heat strengthening rate. The low-temperature polymer forms a different crystal structure and is generally lower in crystallinity. In addition to this structural difference, the end groups of the low-temperature polymer (OH, $CO_2H$) are less reactive than those of the two melt polymers.

The dependence of tensile strength on molecular weight implies that improved properties could be attained by spinning higher molecular weight polymer. Attempts to do this were made by using higher molecular weight polymer obtained from heat strengthened fibers and solid-phase polymerized polymer flake. The results of these spinning experiments are summarized in Table IV. The conditions indicated are those under which the best fibers were obtained. Respinning polymer from heat strengthened fiber (1–4 h at 280 °C) gave fibers with as-spun tensile strengths of about 2 GPa. Although these properties are better than those obtained for lower molecular weight polymer they are substantially below that which would be expected for heat-strengthened fiber of the same molecular weight. Fibers could only be spin at low speeds with little elongation of the fiber resulting in poorly oriented fiber. Increasing spinning speed led to an instability in the threadline. Problems encountered in the spinning of

**Table IV**
**Fiber Properties Obtained with High Molecular Weight Samples**

| sample | $\eta_{inh}$ | spinning speed, m/min | yarn $\eta_{inh}$ | $T/E/M^a$ | comments |
|---|---|---|---|---|---|
| melt polymerized | 0.9 | 900 | 0.9 | 1.5/3/41.4 | uniform fiber |
| heat-treated fibers[b] | | | | | |
| 280 °C/1 h | 1.5 | 90 | 1.5 | 1.9/5/46.9 | uniform fiber |
| 280 °C/4 h | 4.0 | 6 | [c] | 2.2/4/55.2 | uniform fiber |
| solid-phase polymerized flake | | | | | |
| 275 °C/1 h/1 mm | 1.5 | 900 | 1.1 | 1.6/4/56.5 | uniform fiber |
| 275 °C/1 h/1 mm | 1.3 | 350 | 1.5 | 0.8/3/34.5 | thick/thin fiber |

[a] Tensile strength (GPa)/elongation at break (%)/initial modulus (GPa). [b] Fibers were spun by remelting fibers which had previously been heat treated under the conditions indicated. [c] Insoluble.

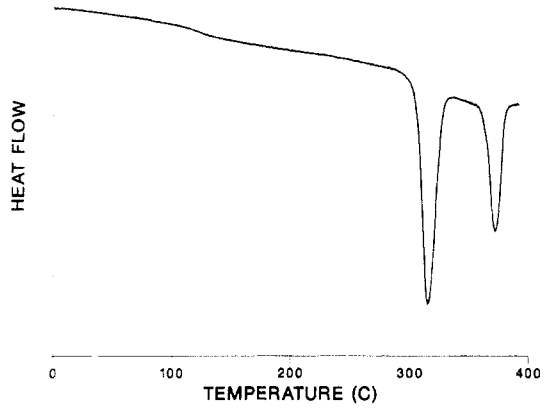


**Figure 11.** DSC scan for solid-phase polymerized 34′PCOPG-T. The crystal to nematic transition is shifted to substantially higher temperature and there is a larger increase in the crystallinity. There is little or no change in the nematic to isotropic transition.

solid-phase polymerized flake were worse. Although this polymer sometimes could be spun at reasonable speeds, as-spun properties were not improved. The relatively poor spinning performance of this polymer results from a difficulty in completely melting the polymer in the press spinning equipment used. In Figure 11 a DSC trace of solid-phase polymerized polymer is shown. There is a dramatic increase in enthalpy and melting temperature after prolonged annealing at high temperature; the sample has increased crystallinity and a higher degree of crystalline perfection. Thus, although the direct spinning of high molecular weight polymer would appear to be an obvious route to improved properties, our efforts to do this were unsuccessful.

A final property studied for 3,4′PCOPG-T fiber was compressive strength. It was hoped that the high level of tensile toughness found for these fibers would be accompanied by an improvement in compressive properties. However, the compressive properties of 34′PCOPG-T are similar to those of other thermotropic polyesters and are significantly worse than those of Kevlar or carbon fiber. As with other highly oriented polymer fibers, compressive failure of 34′PCOPG-T occurs with the formation of kink bands. Compressive properties of 34′PCOPG-T are compared with those of other high performance fibers in Table V.

**Table V**
**Comparison of Compressive Strengths**

| fiber | compressive strength, MPa | fiber | compressive strength, MPa |
|---|---|---|---|
| 3,4′PCOPG-T | 186 | carbon AS-4 | 1440 |
| Kevlar 49 | 365 | Thornel P-55 | 400 |
| PBT | 270 | gel-spun PE | 70 |

**Table VI**
**Meridional Reflections: 3,4′PCOPG-T Fibers**

| | | | thermal history: $d$(obsd), nm | | |
|---|---|---|---|---|---|
| $h$ | $k$ | $l$ | as spun | 190 °C | 280 °C |
| 0 | 0 | 4 | | 1.6900 | 1.6911 |
| 0 | 0 | 8 | | 0.8455 | 0.8456 |
| 0 | 0 | 12 | 0.5639 | 0.5654 | 0.5646 |
| 0 | 0 | 16 | 0.4150 | 0.4185 | 0.4228 |
| 0 | 0 | 20 | 0.3370 | 0.3410 | 0.3382 |
| 0 | 0 | 24 | 0.2819 | 0.2822 | 0.2819 |
| 0 | 0 | 28 | | 0.2407 | 0.2416 |
| 0 | 0 | 32 | 0.2112 | 0.2120 | 0.2114 |
| 0 | 0 | 36 | 0.1880 | 0.1879 | 0.1879 |
| 0 | 0 | 40 | 0.1698 | 0.1690 | 0.1691 |

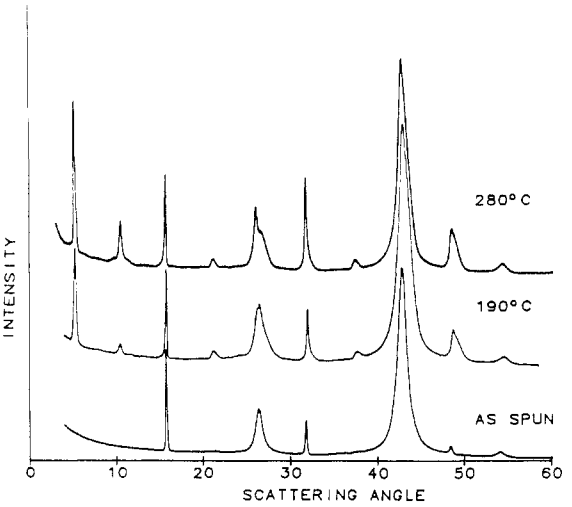


**Figure 12.** Meridional diffractometer scans of 3,4′PCOPG-T fibers. Data for both as-spun and heat-treated fibers are shown. All reflections observed are consistent with a 4-fold helical structure.

**Solid-State Structure.** The X-ray fiber diffraction patterns from single filaments of as-spun 3,4′PCOPG-T fiber and as-spun fiber that had been heat treated at 280 °C for 10 h are shown in Figure 8. The fiber diffraction pattern of the as-spun fiber shows that the fiber has good orientation with no evidence of lateral order or crystallinity. The scattering is characterized by two broad overlapping maxima on the equator ($2\theta$ = 18.6°, 22.4°) and a series of sharp, periodic reflections along the meridian of the diffraction pattern. The scattering is consistent with a quenched nematic structure. Meridional diffractometry scans from these fibers are shown in Figure 12. The meridional reflections, listed in Table VI, can be indexed as orders of a 1.661-nm repeat. This value is consistent with the expected length for the chemical repeat in which the benzophenone segment is in an extended trans conformation. The absence of the 004 reflection may be a consequence of disorder due to the random incorporation

**Table VII**
**Fiber Diffraction Data: 3,4′PCOPG-T**

| unit cell params | scattering condtns, obsd | scattering condtns, Ac2a |
|---|---|---|
| $a$ = 1.251 (2) nm | $hkl$: $k + l = 2n$ | $hkl$: $k + l = 2n$ |
| $b$ = 0.756 (1) nm | $0kl$: $k + l = 4n$; $k, l = 2n$ | $0kl$: $k, l = 2n$ |
| $c$(fiber axis) = 6.765 (6) nm | $h0l$: $l = 2n$ | $h0l$: $l = 2n$ |
| | $hk0$: $h, k = 2n$ | $hk0$: $h, k = 2n$ |
| $\rho$(calcd) = 1.43 g/cm$^3$ | $h00$: $h = 2n$ | $h00$: $h = 2n$ |
| $\rho$(obsd) = 1.38 g/cm$^3$ | $0k0$: $k = 2n$ | $0k0$: $k = 2n$ |
| | $00l$: $l = 4n$ | $00l$: $l = 2n$ |

| $h$ | $k$ | $l$ | $d$-spacing, nm | obsd $d$-spacing, nm | $h$ | $k$ | $l$ | $d$-spacing, nm | obsd $d$-spacing, nm |
|---|---|---|---|---|---|---|---|---|---|
| 2 | 0 | 0 | 0.6255 | 0.6290 | 3 | 1 | 5 | 0.3525 | |
| 0 | 2 | 0 | 0.3780 | | 4 | 1 | 5 | 0.2826 | |
| 2 | 2 | 0 | 0.3235 | | | | | | |
| 4 | 0 | 0 | 0.3128 | 0.3141 | 0 | 0 | 6 | 1.1273 | |
| | | | | | 1 | 0 | 6 | 0.8375 | |
| 1 | 1 | 1 | 0.6441 | 0.6459 | 2 | 0 | 6 | 0.5470 | |
| 2 | 1 | 1 | 0.4807 | 0.4827 | 3 | 0 | 6 | 0.3911 | |
| 3 | 1 | 1 | 0.3646 | | 0 | 2 | 6 | 0.3584 | 0.3576 |
| 4 | 1 | 1 | 0.2887 | | 1 | 2 | 6 | 0.3445 | 0.3433 |
| | | | | | 2 | 2 | 6 | 0.3110 | 0.3108 |
| 0 | 0 | 2 | 3.3820 | | 4 | 0 | 6 | 0.3014 | |
| 1 | 0 | 2 | 1.1733 | | 3 | 2 | 6 | 0.2718 | |
| 2 | 0 | 2 | 0.6151 | | | | | | |
| 3 | 0 | 2 | 0.4139 | | 0 | 1 | 7 | 0.5954 | |
| 0 | 2 | 2 | 0.3757 | 0.3750 | 1 | 1 | 7 | 0.5376 | |
| 1 | 2 | 2 | 0.3598 | 0.3604 | 2 | 1 | 7 | 0.4313 | 0.4300 |
| 2 | 2 | 2 | 0.3220 | 0.3226 | 3 | 1 | 7 | 0.3416 | |
| 4 | 0 | 2 | 0.3114 | | 4 | 1 | 7 | 0.2769 | |
| 3 | 2 | 2 | 0.2971 | | 0 | 0 | 8 | 0.8455 | 0.8455 |
| | | | | | 1 | 0 | 8 | 0.7005 | 0.7007 |
| 1 | 1 | 3 | 0.6219 | 0.6232 | 2 | 0 | 8 | 0.5029 | 0.5026 |
| 2 | 1 | 3 | 0.4713 | 0.4730 | 3 | 0 | 8 | 0.3740 | |
| 3 | 1 | 3 | 0.3604 | 0.3612 | 0 | 2 | 8 | 0.3451 | |
| 4 | 1 | 3 | 0.2867 | | 1 | 2 | 8 | 0.3327 | |
| | | | | | 2 | 2 | 8 | 0.3022 | |
| 0 | 0 | 4 | 1.6910 | 1.690 | 4 | 0 | 8 | 0.2933 | 0.2914 |
| 1 | 0 | 4 | 1.0057 | 1.003 | 3 | 2 | 8 | 0.2659 | |
| 2 | 0 | 4 | 0.5867 | 0.5890 | | | | | |
| 3 | 0 | 4 | 0.4049 | 0.4060 | 0 | 0 | 12 | 0.5637 | 0.5654 |
| 0 | 2 | 4 | 0.3689 | | 0 | 0 | 16 | 0.4228 | 0.4185 |
| 1 | 2 | 4 | 0.3538 | | 0 | 0 | 20 | 0.3382 | 0.3410 |
| 2 | 2 | 4 | 0.3178 | | 0 | 0 | 24 | 0.2818 | 0.2822 |
| 4 | 0 | 4 | 0.3075 | | 0 | 0 | 28 | 0.2416 | 0.2407 |
| 3 | 2 | 4 | 0.2763 | | 0 | 0 | 32 | 0.2114 | 0.2120 |
| | | | | | 0 | 0 | 36 | 0.1879 | 0.1879 |
| 0 | 1 | 5 | 0.6599 | | 0 | 0 | 40 | 0.1691 | 0.1690 |
| 1 | 1 | 5 | 0.5837 | 0.5846 | | | | | |
| 2 | 1 | 5 | 0.4540 | 0.4542 | | | | | |

of the nonsymmetric 3,4′PCOPG segment. The observation of the extended conformation in noncrystalline fibers lends strong support to theories predicting induced rigidity or conformational selection in nematic phases.

Fibers heat treated at 190 °C for 3 h develop substantial crystallinity and have improved orientation (measured crystallite sizes parallel and perpendicular to the fiber axis are 20 and 15 nm, respectively; filament orientation angle is 4.6°) (Figures 8B and 12). The heat-treatment conditions are sufficiently mild that no ester interchange is expected to have taken place. The polymer is semicrystalline; the diffraction pattern has sharp reflections superimposed upon the noncrystalline scattering seen in Figure 8A. On heat treatment under conditions where ester exchange can take place (280 °C) there is a increase in crystallinity that is due to the crystallization of newly formed helical runs, produced by ester interchange.

It is clear that the intensity distribution in this pattern, and therefore the structure of the crystalline component, is different in kind from that of other thermotropic polyesters such the copolymer of *p*-hydroxybenzoic acid and 2-hydroxy-6-naphthoic acid.[24] In these thermotropic polyesters and aramids[25] the diffraction patterns are characterized by strong equatorial and near-equatorial reflections. These strong equatorial reflections are a consequence of the rodlike nature of these polymers. Their absence in our diffraction patterns is a clear indication that 3,4′PCOPG-T is not a simple rodlike molecule. There is also a very notable lack of arcing of the reflections, i.e., the orientation obtained is much higher than would be found in fibers spun from other liquid crystalline polymers.

The positions of 32 reflections in the crystalline pattern were indexed by a orthorhombic unit cell with dimensions $a$ = 1.251 (2) nm, $b$ = 0.756 (1) nm, and $c$(fiber axis) = 6.765 (6) nm. The cell contains 16 chemical moieties and has a calculated density of 1.430 g/cm$^3$, which is in good agreement with the observed density of 1.3812 g/cm$^3$. The indexing of the meridional reflections, shown in Figure 12, is given in table VI. A comparison of observed and calculated $d$-spacings is given in Table VII. Reflections are observed only when certain reflection conditions are met (see Table VII). In a diffraction pattern from a structure with orthorhombic (or lower) symmetry, the reflection conditions expected involving the $00l$ reflections, if present, are the observation of $00l$ reflections only when $l = 2n$. Other classes of reflections would also be governed by reflection conditions involving a $2n$ factor (or no conditions at all). In 3,4′PCOPG-T, $00l$ reflections are observed only

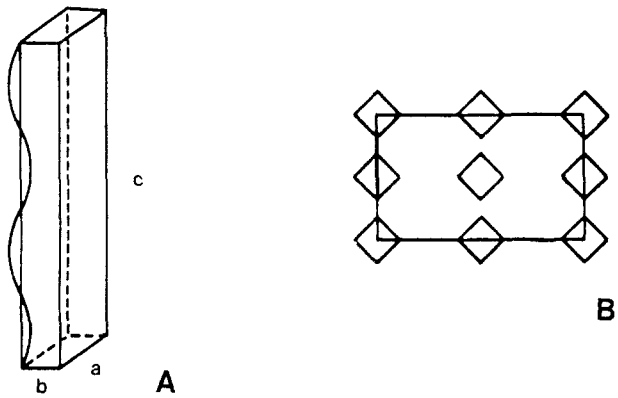


**Figure 13.** (A) The unit cell obtained from fiber diffraction data with the position of one 3,4′PCOPG-T helix indicated. (B) The packing within the unit cell of four 3,4′PCOPG-T chains viewed down the chain axis.

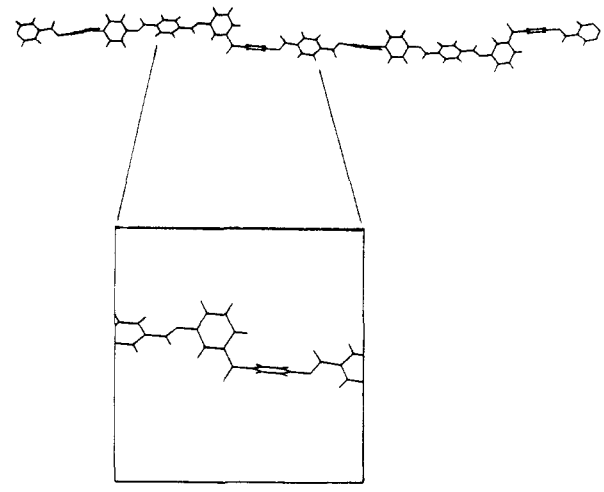

**Figure 14.** Lowest energy chain conformation consistent with the diffraction data.

when $l = 4n$ and other classes of reflections involving $l$, e.g., $0kl$ reflections are observed only when $k + l = 4n$. Since these more stringent diffraction conditions cannot be attributed to space-group symmetry, these "super" conditions must be due to the superposition of molecular symmetry and space-group symmetry. The observation of $00l$ reflections only when $l = 4n$ is the expected scattering condition for a 4-fold helix positioned parallel to the crystallographic $c$ axis. The other super conditions necessarily follow. Thus the molecules in the crystalline component are 4-fold helices with a period of 6.765 nm and a rise per chemical repeat of 1.691 nm. To form this helix the molecule has to be in a nearly fully extended trans conformation and have a head-to-tail sequence. To our knowledge this is the first truly helical structure found for an all-aromatic thermotropic polyester.

The unit cell contains four 4-fold helices. The observation of $hkl$ reflections only when $k + l = 2n$ indicates that the structure is $A$ centered. The space group $Ac2a$ (No. 41) is consistent with the observed scattering conditions and is the most likely space group. Figure 13 shows the positioning of the chains in the unit cell as required by the $Ac2a$ space group. The space group requires the presence of both left- and right-handed helices in the unit cell and that chains of opposite handedness be closer together than chains of like handedness. The nonsymmetric portion of a chain is a single chemical repeat; the remaining contents of the unit cell can be generated by helical and space group symmetry operations.

From structural information from crystal structures of appropriate model compounds[26] and the fiber repeat as determined by the X-ray experiments, models for an isolated 4-fold helical chain were generated by using the Linked Atom Least Squares program.[27] The relative energy of the various models were evaluated after energy minimization. The isolated left-handed chain with the lowest energy is shown in Figure 14. The terephthalate group is incorporated in a manner that allows the carboxyl groups to be trans to each other. In the general chain, models that incorporated trans conformations had less steric compression than those that incorporated cis conformations. The torsional angles that define the conformation of the ester groups are within the range of values observed in small molecules. The phenyl rings in the benzophenone are at approximately right angles to each other, a relative placement often found in small molecules where phenyl groups are separated by a single main-chain atom (e.g., diphenylene thioether[28a] and diphenylmethane[28b] and benzophenone[28c]). The helix can be thought of as a kinked rod. There are straight segments consisting of three phenyl groups separated by 90° kinks that are generated by the keto groups and compensated by the 1,3-phenyl group. There is a mirror-generated right-handed helix with equal energy. The complete structure is under study and will be reported when complete.

**Table VIII**
**Observed $d$-Spacings: Low-Temperature Structure**

| layer line | $d$-spacing, nm | layer line | $d$-spacing, nm |
|---|---|---|---|
| $hk0$ | 0.500 | $hk4$ | 0.565 |
| | 0.315 | $hk5$ | 0.480 |
| $hk1$ | 0.383 | | 0.405 |
| $hk2$ | 0.560 | | 0.307 |
| $hk3$ | 0.330 | $hk6$ | 0.344 |
| | 0.379 | | 0.324 |

Melt polymerization was used to prepare the polymer described so far. Under these conditions we expect that T-34′-T (up) and T-43′-T (down) segments are incorporated randomly into the chain. The presence of sharp meridional reflections in the as-spun fiber is not inconsistent with this expectation, since both up and down segments have the same projection on the fiber axis in the trans conformation. Heat treatment at 190 °C produces a semicrystalline diffraction pattern consistent with head-to-tail segments crystallizing and chain segments with a random sequence not. This model would explain the oriented noncrystalline component in the fiber. The crystalline correlation length of 20 nm for the 004 reflection indicates that crystallizable runs of at least 12 chemical repeats exist in as-spun polymer.

Low-temperature solution polymerization results in a polymer with a second crystal form. Fibers were melt-spun by a procedure similar to that used for the melt-polymerized material. The as-spun fiber, in contrast to fibers prepared from melt-polymerized polymer, is semicrystalline. After annealing at 190 °C, the crystalline perfection increases somewhat. The fiber diffraction pattern from such a fiber is shown in Figure 15A. The crystalline component has a very different structure than found in the melt-polymerized material. The $d$-spacings of the reflection found in this pattern are listed in Table VIII. We have been unable to index this diffraction pattern. However, the reflections appear to lie on layer lines that can be indexed as orders of a ca. 3.5-nm spacing which, by analogy to the other structure, corresponds to two extended chemical moieties in the fiber repeat.

Figure 15B shows a diffraction pattern from a fiber of low-temperature polymerized polymer that has been heat

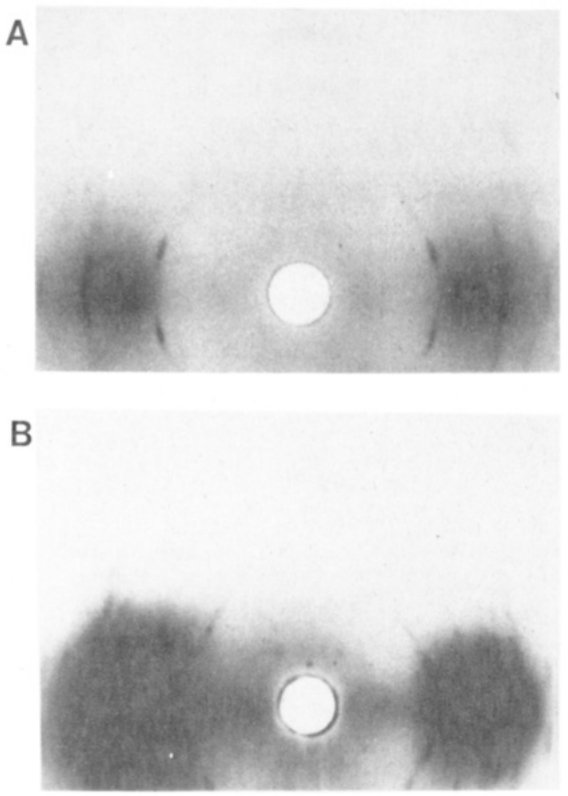


**Figure 15.** (A) Fiber diffraction pattern obtained from as-spun 3,4′PCOPG-T fiber prepared from low-temperature solution-polymerized polymer. The fiber is semicrystalline with a different crystal structure than that found for melt-polymerized material. (B) The diffraction pattern found after heating at 280 °C for 4 h. The diffraction pattern now contains reflections due to both crystal structures. For both patterns the fiber axis is vertical.

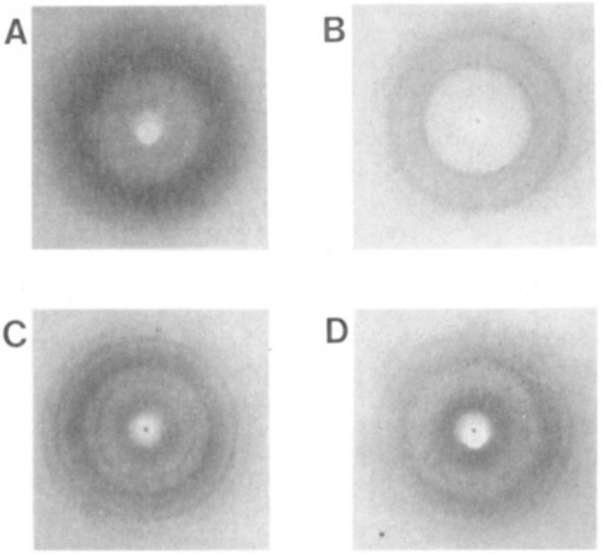


**Figure 16.** Powder patterns obtained from a melt-polymerized flake prepared by the two polymerization schemes. The melt-polymerized flake (A) is converted to a semicrystalline form (C) by heating (30 min at 290 °C, 5 h at 190 °C). The reflections observed are those expected for the crystal structure associated with the 4-fold helical conformation. In contrast, the as-prepared solution-polymerized material (B) is semicrystalline with a second crystalline form. Heating under the same conditions (D) yields a mixture of the two phases.

treated at 280 °C for 4 h. Superimposed on the diffraction pattern of the low-temperature phase (Figure 15A) are features from the diffraction pattern of the 4-fold helical structure and an increased amorphous contribution. Eventually, with prolonged annealing times, the diffraction features associated with the low-temperature polymerization polymer completely disappear leaving a pattern very similar to that shown in Figure 8B. A similar behavior is observed when polymer flake is examined. Figure 16A,B shows the powder diffraction patterns of as-polymerized polymer. The melt-polymerized material is amorphous while the low-temperature polymerized material is semicrystalline. Figure 16C,D shows the same samples after exposure to identical annealing conditions (30 min at 290 °C followed by 5 h at 190 °C). The melt-polymerized material has crystallized to give the diffraction pattern associated with crystals containing the 4-fold helical form of the polymer. The low-temperature material has a diffraction pattern that has features of both crystalline forms.

While there are two chemical repeats in the fiber repeat, there is no crystallographic evidence (002 reflection) for a regular helix. Thus the two chemical moieties in the fiber repeat are crystallographically nonequivalent. One likely source for the difference between melt- and solution-polymerized material is the manner in which units are incorporated. In polymer produced by high-temperature melt polymerization a random distribution of "up" and "down" segments within a given chain is expected. On the other hand at low temperature, where ester interchange does not occur, the difference in reactivity between the 3- and 4′-hydroxyls is enhanced and could lead to a more regular incorporation of monomers. It is also observed that polymerization is accompanied by phase separation. Evidence that the difference in crystallization characteristics of material prepared by different polymerization routes is related to sequence distribution is inferred from high-temperature annealing studies.

## Conclusions

The conformations accessible to the 3,4′PCOPG-T chain result in a number of unique properties. The phase behavior of the polymer is one obvious example. A sharp nematic to isotropic transition has rarely been found for all-aromatic main-chain nematic polymers. In contrast to other monomers which are used to obtain rodlike chains, 3,4′PCOPG-T monomer has conformations which result in considerable flexibility. Thus the chain can easily adopt a flexible conformation in an isotropic phase. Conformational selection or induced rigidity in the nematic phase results in the exclusion of the flexible cis conformation and produces the desired extended conformation in the nematic phase. The importance of induced rigidity in 3,4′PCOPG-T phase transitions is consistent with theoretical predictions[5] and is supported by experimental evidence including DSC results for transition entropy and X-ray studies of as-spun fibers.

This type of flexibility does not occur in 1,4-linked aromatic polymers. The para-substituted monomers have a conformation which under all circumstances deviates only slightly from a rodlike conformation. The flexibility of the chain can be modified by the addition of nonconforming monomers, e.g., 1,3-linked aromatics, but these monomers increase the flexibility of the chain even in the nematic phase since there is no way in which the conformation can become rodlike.

Because of the nonsymmetric nature of the 3,4′PCOPG residue, the diol can be thought of as having a head and a tail. Three types of sequence are important: head-to-tail, head-to-head, and random. The melt-polymerized 3,4′PCOPG-T has an effectively random incorporation of the diol. This conclusion is based on the observation of the diffraction pattern characteristic of the head-to-tail structure in fibers heat treated at 190 °C and the presence

of a crystallization endotherm at 200 °C in melt-spun material. In contrast, the diol in low-temperature (solution) polymerized polymer appears to be incorporated largely in a head-to-head fashion.

Solid-phase polymerization results in a stable polymer configuration in which the diol is incorporated in a head-to-tail fashion. This configuration is characterized by a 4-fold helical structure. This structure is seen in all samples held at temperatures where ester interchange takes place, regardless of the sequence in the as-polymerized material.

The presence of an extended structure in the nematic phase has important consequences in terms of fiber properties. As-spun fibers have properties which are similar to those obtained from rodlike chains because of this extended structure. The disorder present due to the random incorporation of the diol prevents the formation of large crystallites so that relatively low melting temperatures are found. This has important consequences in that processing temperatures compatible with commercial polyester equipment can be used. High-temperature heat treatment results in fiber tensile properties which are comparable to the best reported for melt-spun fibers. The orientation of these fibers is much higher than generally found for rodlike thermotropic polyesters so that a higher percentage of the ultimate properties is obtained. It is likely that the flexibility of the chain due to the possibility of assuming the cis conformer allows the removal of defects either in spinning or during crystallization.

**Registry No.** (3,4′-PCOPG diacetate)(T) (copolymer), 75737-94-9; (3,4′-PCOPG diacetate)(T) (SRU), 75796-78-4; (3,4′-PCOPG)(diphenyl terephthalate) (copolymer), 117653-46-0; (3,4′-PCOPG)(terephthaloyl chloride) (copolymer), 117653-47-1.

## References and Notes


(1) Flory, P. J. *Proc. R. Soc. London, Ser. A* **1956**, *234*, 73.
(2) (a) Finkelman, H. In *Polymer Liquid Crystals*; Ciferri, A., Krigbaum, W. R., Meyer, R. B., Eds.; Acadmic Press: New York, 1982; Chapter 2. (b) Cifferi, A. Ibid.
(3) Schaefgen, J. R.; Bair, T. I.; Ballou, J. W.; Kwolek, S. L.; Morgan, P. W.; Panar, M.; Zimmerman, J. In *Ultra-High Modulus Polymers*; Cifferi, A., Ward, I. M., Eds.; Applied Science Publishers: London, 1977; Chapter 7.
(4) Hummel, J. P.; Flory, P. J. *Macromolecules* **1980**, *13*, 479. Erman, B.; Flory, P. J.; Hummel, J. P. *Macromolecules* **1980**, *13*, 485.
(5) Pincus, P.; de Gennes, P.-G. *Polym. Prepr. (Am. Chem. Soc., Div. Polym. Chem.)* **1977**, *18*, 161. Kim, Y. H.; Pincus, P. *Biopolymers* **1979**, *18*, 2315. Matheson, R. R.; Flory, P. J. *J. Phys. Chem.* **1984**, *88*, 6606. Matheson, R. R. *Macromolecules* **1986**, *19*, 1286.
(6) Irwin, R. S. U.S. Patent 4,245,082 (issued to Du Pont).
(7) The results reported in this paper include both results for the homopolymer and a copolymer containing 2.5% resorcinol. We have found no difference between the properties of the two compositions.
(8) Gardner, K. H.; Hilmer, R. M. Unpublished results.
(9) Alexander, L. E. *X-ray Diffraction Methods in Polymer Science*; Kreiger: New York, 1979; Chapter 5.
(10) Allen, S. R. *J. Mater. Sci.* **1987**, *22*, 853.
(11) The Mark–Houwink coefficient should actually be determined by using intrinsic viscosities. Use of inherent viscosity results in a measured power low exponent that is somewhat larger than the correct value.
(12) See, for example: Dewar, M. J. S.; Griffin, A. C. *J. Am. Chem. Soc.* **1975**, *97*, 6662. Young, W. R.; Haller, I.; Green, D. C. *J. Org. Chem.* **1972**, *37*, 3707.
(13) Yoon, D. Y.; Bruckner, S.; Volksen, W.; Scott, J. C.; Griffin, A. C. *Faraday Discuss. Chem. Soc.* **1985**, *79*, 41.
(14) The rheological properties of 3,4′PCOPG-T have been compared to those of other polyesters which have nematic to isotropic transitions in: Wunder, S. L.; Ramachandran, S.; Gochanour, C. R.; Weinberg, M. *Macromolecules* **1986**, *19*, 1696.
(15) For some temperatures the data did not quite cover the entire range from 100 to 10 000 $s^{-1}$. In these cases the value for either 100 or 10 000 $s^{-1}$ was obtained by extrapolation using a linear least-squares fit.
(16) Matheson, R. R. *Macromolecules* **1980**, *13*, 643.
(17) Papkov, S. P.; Kulichikhin, V. G.; Kalymykova, V. D.; Malkin, A. Y. *J. Polym. Sci., Polym. Chem. Ed.* **1974**, *12*, 1953.
(18) de Gennes, P.-G. *The Physics of Liquid Crystals*; Oxford University Press: London, 1974.
(19) Prevorsek, D. C. In *Polymer Liquid Crystals*; Ciferri, A., Krigbaum, W. R., Meyer, R. B., Eds.; Academic Press: New York, 1982; Chapter 12.
(20) Luise, R. R.; Kwolek, S. L. *Macromolecules* **1986**, *19*, 1789.
(21) Zimmerman, J. Unpublished results.
(22) Lenz, R.; Jin, J. I.; Feichtinger, A. *Polymer* **1983**, *24*, 327.
(23) Luise, R. R. U.S. Patent 4,183,895 (issued to Du Pont, 1980).
(24) Blackwell, J.; Biswas, A.; Bonart, A. *Macromolecules* **1985**, *18*, 2126 and references therein.
(25) Northolt, M. G. *Eur. Polym. J.* **1974**, *10*, 799.
(26) Iball, J.; MacKay, K. J. H. *Acta Crystallogr.* **1962**, *15*, 148; Adams, J. M.; Morsi, S. E. *Acta Crystallogr.* **1976**, *B32*, 1345; Kaiser, J.; Richter, R.; Lemke, G.; Golic, L. *Acta Crystallogr.* **1980**, *B36*, 193.
(27) Smith, P. J. C.; Arnott, S. *Acta Crystallogr.* **1976**, *A34*, 3.
(28) (a) Vijayalakshmi, B. K.; Srinivasan, R. *J. Cryst. Mol. Struct.* **1973**, *3*, 147. (b) Gardner, K. H.; Blackwell, J. *Acta Crystallogr.* **1972**, *B36*, 1988. (c) Fleisher, E. B.; Sung, N.; Hawkinson, S. *J. Phys. Chem.* **1968**, *72*, 4311.


# A Novel Nonionic Hydrogel from 2-Methyl-2-oxazoline


**Yoshiki Chujo, Yutaka Yoshifuji, Kazuki Sada, and Takeo Saegusa***

*Department of Synthetic Chemistry, Faculty of Engineering, Kyoto University, Yoshida, Sakyo-ku, Kyoto 606, Japan.*

*Received April 20, 1988*


ABSTRACT: A novel nonionic hydrogel consisting of poly(*N*-acetylethylenimine) was prepared from 2-methyl-2-oxazoline. Partial alkaline hydrolysis of poly(*N*-acetylethylenimine) was followed by a cross-linking reaction with hexamethylene diisocyanate to produce a gel. The cross-linking reaction proceeded quantitatively in bulk. By use of 1,8-diazabicyclo[5.4.0]undec-7-ene as a catalyst in *N*,*N*-dimethylformamide, the gel was produced under mild conditions. The resulting dried gel was immersed in water to form a stable hydrogel. The water uptake was in up to 72 multiples of the weight of dried gel. This nonionic hydrogel showed also quite a high swelling property in aqueous salt such as 5% aqueous NaCl. The remaining secondary amino groups in the gel after the cross-linking reaction with a diisocyanate influenced the swelling property in water, which could be successfully eliminated by reaction with ethyl isocyanate.


## Introduction

Hydrogels have been widely used in a number of applications, e.g., sanitary materials, cosmetics, ingredients for paints or adhesives, food packing, water-holding agents in horti- or agriculture, sealing or packing materials in civil engineering, and some medical applications such as contact lenses[1] or slow-release devices. However, the hydrogels so far depend on carboxylic or sulfonic acids salts as hydrophilic group and, hence, generally do not have satisfactory characteristics toward aqueous salt. Nonionic hydrogels

0024-9297/89/2222-1074$01.50/0 